

# Exploring the Effects of Spatial Constraints and Curvature for 3D Piloting in Virtual Environments




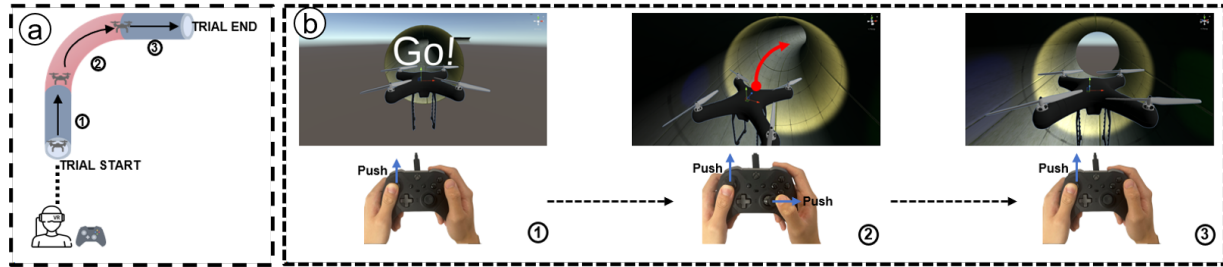
Xuning Hu<sup>1\*</sup> Xinan Yan<sup>1\*</sup> Yushi Wei<sup>2</sup> Wenxuan Xu<sup>3</sup> Yue Li<sup>1</sup> Yue Liu<sup>4</sup> Hai-Ning Liang<sup>2</sup>  <sup>†</sup><sup>1</sup> School of Advanced Technology, Xi'an Jiaotong-Liverpool University, Suzhou, China<sup>2</sup> Computational Media and Arts Thrust, The Hong Kong University of Science and Technology (Guangzhou), Guangzhou, China<sup>3</sup> Guarini School of Graduate and Advanced Studies, Dartmouth College, Hanover, USA<sup>4</sup> School of Optics and Photonics, Beijing Institute of Technology, Beijing, China

Figure 1: (a) In the virtual reality simulation, a participant pilots an aircraft through a tunnel characterized by constraints on width and height using a game controller. Circles labeled 1, 2, and 3 indicate the successive positions of the aircraft as it navigates through the tunnel. (b) The participant executes a sequence of maneuvers using dual joysticks on the game controller to pilot the aircraft along the prescribed tunnel path.

## ABSTRACT

Piloting requires users to control and navigate the aircraft within a designated pathway, with a controller that utilizes two joysticks to control the aircraft. This task is representative of various daily and gaming scenarios, such as controlling the aircraft to capture the photo or navigating an object in a game from the start position to the end via a trajectory. In this work, we explore a model (based on the Steering Law) that predicts the piloting time required in spatial-constrained environments. Thus, two user studies are conducted to help us understand the relationship between path complexity (curvature) and spatial constraints (width and height). According to the results, we propose a model that can achieve 52.6% and 60.6% improvement in R-square and the Akaike Information Criterion (AIC), respectively. Next, an additional study was conducted to further verify the performance and efficiency of our proposed model with the change of movement direction and orientation. Our model and experimental results can benefit both game and interface designers of applications that require controlling moving objects along specific trajectories in virtual reality environments.

**Index Terms:** Virtual Reality, Game Controller, Steering Law, Graphical User Interfaces, Modeling, Navigation

## 1 INTRODUCTION

Steering, navigating an object from its start to the end along a predefined path/trajectory, is one of the fundamental tasks in our daily life. Previous works have shown that steering behavior and performance, such as the overall task duration, can be accurately predicted using mathematical models known as Steering Law [2].

\*These authors contributed equally to this work.

<sup>†</sup>Corresponding author (e-mail: hainingliang@hkust-gz.edu.cn)

The model's applicability has been validated in various scenarios and with different devices, including 2D touch screens with bare hands [31], 3D steering with hand-held controllers [21], and 3D driving tasks using driving simulators [39, 38]. The fundamental concept of the Steering Law is that the attributes of the predetermined steering path, such as its length and width, have a significant and direct impact on the user's performance and behavioral patterns. In detail, a wider and shorter trajectory tends to result in a shorter completion time for the task [36, 2].

While numerous extended Steering Laws have been proposed and applied to various complex scenarios, there is a lack of studies that consider spatial constraints such as width and height separately in real 3D virtual environments. Specifically, to the best of our knowledge, the only steering-based study investigating the impact of spatial constraints on user behavior while independently considering width and height was conducted utilizing a large 2D display, which simulates 3D height visually on a flat screen [15]. Given the difference in interactivity between simulated (2D screen) and real/immersive 3D scenarios, users receive different visual perceptions, leading to distinct interaction strategies [16]. Consequently, we cannot directly apply the findings from this study to real/immersive 3D environments [33]. More commonly, in 3D-based steering tasks, previous studies have typically assumed that the width and height of the steering tunnel (3D path/trajectory that users need to steer) are equal or the height is negligible [22, 38, 5]. However, With the increasing complexity of interaction tasks and the maturity of virtual reality (VR) based technologies, immersive and high-fidelity 3D-based interactions are gaining significance. In these environments, the different levels of spatial constraints have been demonstrated to significantly impact users' perception and interactive strategy [26]. A typical task within such scenarios is aircraft piloting, including real-life drone operations or engaging in fighter games in VR [19, 6]. Thus, the findings of prior studies that did not take height into account may not be directly applicable to scenarios where width and height are inequalities.

In this work, three user studies centered on piloting tasks with

third-person perspectives, which are typical in AR- and VR-based interactions [25, 23, 24, 20], were conducted to gain a deeper understanding of the influence of spatial constraints (width and height) on user behavior and performance in immersive VR environments. Additionally, we introduced curvature as an additional factor to simulate task complexity. Within the first study, we designed a straight tunnel with varying widths, heights, and lengths (where the curvature radius approaches infinity). Our findings illustrated the disproportionate impact of width and height. Thus, we designated the primary influential factor as the major effect axis while identifying the secondary factor as the minor effect axis (see Sec. 4). Subsequently, the second user study was conducted to assess the relative importance of width and height across various levels of task difficulty, represented by different curvature radii. Our empirical findings revealed that the weight assigned to the minor effect axis fluctuated in accordance with the Log-normal distribution curve (see Sec. 5). Based on these results, we proposed an extended Steering Law model aimed at elucidating and predicting behavioral patterns and estimating the duration required for steering across different combinations of width, height, length, and curvature radius (See Sec. 6). The outcomes suggest that our model outperformed at 52.6% and 60.6% in terms of AIC and R-square compared to the previous model. Finally, the third study was used to further verify our proposed model by revising the curvature radius, piloting direction, and orientation (See Sec. 7). The results consistently indicate that our model maintains a high fit with strong capabilities in parsing user behavior.

In summary, our primary contributions include: (1) Validated the applicability of the Steering Law in 3D piloting tasks. (2) The empirical demonstration of the difference in weighting between width and height, highlighting the varying importance of width and height on user behavior in the piloting task, reveals inconsistencies. (3) Examining the correlation between curvature radius and the trend of weighted values for width and height, the weighted values maintain consistency with the Log-normal distribution curve where the curvature radius increases. (4) Proposing a novel extended Steering Law model capable of predicting piloting duration and interpreting behavioral patterns, providing a reference for future game or interface designers to evaluate task difficulty and interface suitability.

## 2 RELATED WORK

### 2.1 Steering Law with Width, Height, and Curvature Radius

The Steering Law primarily focuses on interpreting the behavioral patterns and performance of individuals in steering tasks. These tasks involve users navigating objects or themselves through paths constrained by width and limited length [4, 38]. Behavior and performance are typically represented by the metric of movement time ( $MT$ ), which refers to the time required to steer from the start to the end point [2]. The relationship between  $MT$  and width ( $W$ ) and length ( $A$ ) can be expressed [2]:

$$MT = a + b \int_c \frac{ds}{W(s)} \quad (1)$$

where  $a$  and  $b$  represent empirical constants,  $s$  denotes a specific position along path  $c$ , and  $W(s)$  refers to the width at the position  $s$ . Eq. (1) can be further simplified by assuming that path  $c$  maintains the width consistently:

$$MT = a + b \frac{A}{W} \quad (2)$$

Thus, the  $ds$  and  $W(s)$  can be replaced by the independent value of path length  $A$  and constant width  $W$ . Notably, the intercept of  $a$  has been empirically demonstrated that can be removed by previous

work [36, 28, 10]. Therefore, according to the law of  $MT = \frac{A}{V}$ , the average movement speed ( $V$ ) can be formulated as:

$$V = bW \quad (3)$$

More relevant to our work, previous research has primarily focused on 2D screens where the steering path is constrained solely by width or in 3D environments where the width and height are set as equal values [35, 37, 22, 34]. Given spatial constraints, which encompass both width and height, are commonly used in 3D complex interactive tasks such as aircraft photography and game control. Those aforementioned models that solely consider width constraints might not be applied to scenarios where width and height differ. At present, the only study that has explored spatial constraints related to height and width was conducted by Kattinakere et al. [15], who simulated visual height perception on a 2D screen and proposed an extended Steering Law model based on their results:

$$MT = a + b \sqrt{\eta \left( \frac{A}{H} \right)^2 + \left( \frac{A}{W} \right)^2} \quad (4)$$

where  $\eta$  denotes the weighting value assigned to height determined through regression, while the weight value for width defaults to 1. The introduction of  $\eta$  enhances the model's predictive capacity for  $MT$  within scenarios featuring existing spatial constraints. However, the model's applicability still needs to be verified further due to two concerns: (1). The model was constructed based on results obtained from a simulated 3D environment, which differs from the current immersive/high-fidelity 3D scenario due to variations in interactive characteristics [26]. (2). The model only considered the condition where the predefined steering trajectory was straight, leaving its capabilities unexplored in more complex scenarios, such as varying curvature radius ( $R$ ).

The curvature radius refers to the extent of the curve of the steering path, where larger values represent a straighter trajectory. Numerous studies have confirmed that the  $R$  can significantly influence users' steering performance, impacting both the  $MT$  and  $V$  [27, 36]. For example, Montazer et al. [27] demonstrated the linear relationship between  $R$  and  $V$ , where larger  $R$  values correspond to faster speed  $V$ . In addition, their work also identifies an interaction effect between  $W$  and  $\frac{1}{R}$ . Thus, the model can be expressed as Eq. (5). The  $a$ ,  $b$ ,  $c$  and  $d$  are empirical values.

$$V = a + b \cdot W + c \cdot \frac{1}{R} + d \cdot W \cdot \frac{1}{R} \quad (5)$$

Taking cues from Montazer et al.'s findings [27], Yamanaka and Miyashita [36] introduced a novel model designed to predict  $MT$  across diverse path features, including width, length, and curvature radius (See Eq. (6)). While the model demonstrated strong capabilities in predicting  $MT$ , it still lacks the ability to interpret behavior generated under conditions of spatial constraint.

$$MT = a + b \cdot \frac{A}{W + c \cdot \frac{1}{R} + d \cdot W \cdot \frac{1}{R}} \quad (6)$$

### 2.2 Piloting Aircraft and Spatial Constraints

Piloting aircraft along a predetermined trajectory has wide applications across various domains, such as drone photography [32], agricultural spraying [32], and VR aerial gaming or training [30]. Nevertheless, during piloting, a myriad of unforeseen circumstances often arise, such as challenges in effectively adhering to the designated path or collisions between aircraft and obstacles. Prior research has mainly attributed such occurrences to two factors: (1) the flight path designed is considered unreasonable or excessively challenging [13], and (2) discrepancies or deficiencies in the pilot's spatial perception concerning height and width [11, 12].

Therefore, understanding how to effectively design flight trajectories while assessing their interactive difficulty and comprehending individuals' perceptions of width and height during a piloting task becomes significant. While previous studies have not specifically investigated the relationship between flight trajectories and spatial constraints encountered during flight, strategies employed in human locomotion may offer relevant insights. For instance, Cohen et al., [7] have suggested that visual uncertainty and motor noise contribute to individuals maintaining a greater safety margin while walking. Similarly, Kiefer et al. [16] observed that participants adjust their flight trajectories by altering the positioning of visual cues when encountering spatial restrictions in their path. Even when the limitations of the interactive space are no longer highly restrictive, users may continue to adhere to this heightened adjustment habit as a safety strategy.

While the aforementioned studies allow for some intuitive inferences to be made, such as the possibility that a heightened and broader spatial interactive space might enhance user performance, they do not systematically elucidate the relationship between the spatial constraints of the path, its complexity, and the corresponding user performance and behavior. Therefore, in this work, we systematically examined the relationship between spatial constraints and complexity of the trajectory, as well as user behaviors within the context of piloting, elucidating the performance of users across different path characteristics by employing mathematical modeling.

### 3 RESEARCH QUESTION

Drawing from the literature discussed earlier, one can see that there persists a gap in our comprehension regarding the correlation between user behavioral patterns and the characteristics of the piloting path, encompassing factors like width, height, length, and curvature, particularly in the context of piloting control. Thus, to better understand user behavior patterns and the applicability of existing models in piloting control tasks, four research questions (RQ) were formulated:

**RQ1:** *Can the performance of piloting control be modeled using the Steering Law?* Several studies have demonstrated that the Steering Law can effectively predict the total time spent in various navigation tasks, such as walking [29] and driving [39, 38]. However, the applicability of this law to piloting control tasks remains uncertain, particularly given the enhanced dimensions (upward and downward) and degrees of control freedom (pitch, roll, and yaw) inherent in piloting as opposed to driving or walking. Therefore, further exploration is necessary to determine whether the Steering Law can adequately model behavior in this context.

**RQ2:** *Can user behavior and performance in piloting control tasks be influenced by the height and width of the tunnel?* Previous work proposed that tunnel width and height can significantly influence users' steering performance in a simulated 3D stylus-based task [15]. However, given the differences in interactive environments (2D vs. 3D), devices (display vs. HMD), tasks (pen steering vs. piloting control), and methods (stylus vs. game controller), the influence of varying width and height on users' performance and behavior in piloting control tasks remains unexplored.

**RQ3:** *Do width and height have different effects on user behavior when the tunnel is curved?* While the impact of tunnel width and height on user behavior and performance has been identified in 3D large screen [15], the findings mainly pertain to scenarios involving steering through straight tunnels. However, many studies have shown that within 2D steering tasks, there are interaction effects between tunnel width and curvature radius [27, 36]. Therefore, when examining the influence of tunnel width and height on users, it is insufficient to focus on the scenario of only a straight piloting trajectory. Thus, in this study, it is important to integrate various curvature radii into the tunnel characteristics to comprehend the impacts of width and height thoroughly.

**RQ4:** *If width and height exhibit varying effects at different radii of curvature, could a new model be proposed to elucidate this behavioral pattern?* If we can confirm the interaction effects between curvature radius and tunnel width and height, as described in RQ3, we also aim to propose an extended Steering Law model capable of elucidating the effects of width and height under various curvatures within the context of piloting control. This model can provide a more comprehensive understanding to game and interface designers.

## 4 USER STUDY 1: STEERING LAW VERIFICATION AND WIDTH AND HEIGHT ANALYSIS

The primary goal of the first study was to validate the applicability of the Steering Law on piloting control tasks (RQ1) and examine the effects of tunnel width and height on users' behaviors and performances (RQ2). To this end, data was collected from participants while they were required to wear a VR HMD to control an aircraft through an uncurved and constrained tunnel.

### 4.1 Participants

Sixteen participants (4 female, 12 male), ages between 19 and 26 ( $M = 21.31$ ,  $SD = 2.08$ ), were recruited from a local university. All participants had normal or corrected-to-normal vision and reported they could see all objects in the scene clearly. All participants were right-handed. Five participants reported using VR devices for 0-5 hours per week, six for 5-10 hours, and three had never used VR devices before. Additionally, all participants had prior experience using controller-based methods to pilot the aircraft in the game.

### 4.2 Simulator and Apparatus

The experimental program was developed using Unity3D and integrated with the DroneSimPro plugin [1], a professional piloting simulation software engineered to provide lifelike flight experiences. This integration allowed us to simulate the aircraft's physical movement more realistically. The program was run on an Intel Core i9 processor PC with an NVIDIA RTX 3080 Ti graphics card. Participants performed the experiment with an Oculus Quest Pro headset (featuring  $1800 \times 1920$  resolution per eye). The aircraft was navigated using an Xbox One game controller, with two joysticks employed for different functions: the right joystick controlled forward/backward/left/right movement, while the left joystick managed altitude and orientation. This control mechanism was chosen to emulate mainstream devices currently available on the market, ensuring the validity of the experimental results [9, 8].

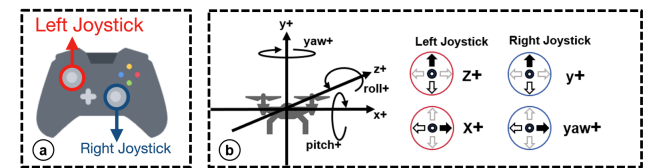


Figure 2: The Xbox controller with Left Joystick and Right Joystick. (b) The Left Joystick controls the aircraft's forward and backward movements (Z-axis) and panning left and right (X-axis). The Right Joystick controls the aircraft's upward and downward movements (Y-axis), as well as turning left and right (Yaw-axis).

### 4.3 Task

In this study, we employed experimental setups akin to those in earlier research studies [18, 38]. Participants, wearing VR headsets and holding Xbox controllers, were seated to navigate virtual aircraft through a tunnel that included three parts: a 50-meter starting area, a measurement area, and a 50-meter ending area [38]. Data

collection was confined to the measurement area, with its length predetermined by the experimental setup (See Fig. 3 C). During the piloting operation, participants were instructed to avoid any collision between the aircraft and the inner walls of the tunnel. The trial was considered unsuccessful in the event of a collision, and participants received auditory feedback signaling task failure. Subsequently, they were required to repeat the entire trial until successful navigation was achieved. As with other studies on the Steering Law [3, 17], participants were instructed not to remove their hands from the controller while steering the aircraft nor allow the aircraft to hover within the tunnel. Additionally, they were required to balance speed and accuracy throughout the task.

#### 4.4 Design and Procedure

The experiment employed a  $3 \times 3 \times 2$  within-subjects design with three independent variables: Effective Widths ( $W$ ): 1m, 1.5m, and 2m, Effective Heights ( $H$ ): 1m, 1.5m, and 2m, and Movement Distances ( $A$ ): 50m, 100m, leading to 18 experimental conditions:

Consistent with the approach taken by Yamanaka et al., [38], we did not directly use the height and width of the tunnel to represent the final values. Instead, we employed the concept of effective width ( $W$ ) and height ( $H$ ). Specifically, the effective width is determined by subtracting the width of the aircraft from the width of the tunnel, while the effective height is calculated using a similar approach (see Fig. 3 A and B). The movement distances ( $A$ ) were determined by the actual length of the measurement area. It is important to note that in this study, our focus was to verify the applicability of the Steering Law in 3D third perspective piloting-based tasks and to assess the effect of tunnel width and height on user behavior and performance. Therefore, we only considered the scenario where the tunnel is straight, i.e., the curvature radius approaches infinity.

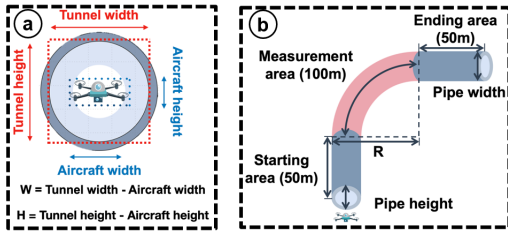


Figure 3: (a) Describes the calculation methods for effective width and height; (b) Describes the specific measurement details and information about the aircraft turning right.

To mitigate the potential learning effect, we implemented a Latin square design in our user study. Specifically, we counterbalanced the path length  $A$  first. Then, each level of  $H$  was counterbalanced accordingly. Finally, within each level of  $H$ , the order of  $W$  was arranged using a Latin square. After the experiment, a total of 864 successful trials ( $3 W \times 3 H \times 2 A \times 3 \text{ repetitions} \times 16 \text{ participants}$ ), each encompassing data on movement time ( $MT$ ) and average movement speed ( $V$ ), were collected.

Before the experiment, participants completed a demographic questionnaire. Following this, they were introduced to the VR headset and controller, with experimenters explaining the task requirements. After the introduction, assistance was provided to ensure proper headset adjustment. A 5-minute practice session followed to acquaint participants with the piloting control mechanism and task specifics. Subsequently, the formal experiment was commenced, lasting about 25 minutes. Although breaks between trials were permitted, none of the participants opted to take one.

#### 4.5 Results

From the experiment, we collected 920 records, including 864 successful trials and 56 failed trials, resulting in an error rate of 12%. Before analyzing the successful trials, 62 trials (7%) of outliers were removed in which the movement time or average movement speed was above or below three standard deviations from the mean values ( $mean \pm 3std.$ ) in each condition. Then, we ran the repeated-measures ANOVA (RM-ANOVA) tests to analyze the movement time and average movement speed. The Greenhouse-Geisser was employed to adjust the degree of freedom if the assumption of sphericity was unmet. The Bonferroni corrections were adopted for post-hoc pairwise comparisons.

##### 4.5.1 Movement Time

We found significant main effects for  $A$  ( $F_{1,15} = 1035.183, p < 0.001, \eta^2 = 0.661$ ),  $W$  ( $F_{2,30} = 72.980, p < 0.001, \eta^2 = 0.218$ ), and  $H$  ( $F_{2,30} = 4.753, p = 0.009, \eta^2 = 0.016$ ) (See Fig. 4). Significant interactions were found for  $A \times W$  ( $F_{2,30} = 52.794, p < 0.001, \eta^2 = 0.906$ ),  $A \times H$  ( $F_{2,30} = 27.401, p < 0.001, \eta^2 = 0.684$ ),  $W \times H$  ( $F_{4,60} = 2.839, p = 0.025, \eta^2 = 0.245$ ),  $A \times W \times H$  ( $F_{4,60} = 5.814, p < 0.001, \eta^2 = 0.943$ ).

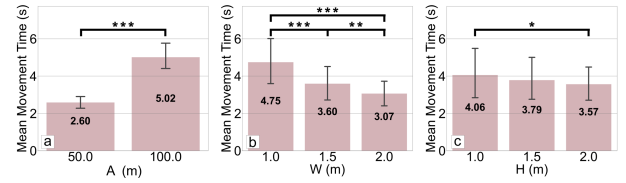


Figure 4: Movement times for each parameter. The error bars show 95% CIs(\* $p < 0.05$ , \*\* $p < 0.01$ , \*\*\* $p < 0.001$ )

##### 4.5.2 Average Movement Speed

The significant main effects in terms of the average movement speed were found for  $W$  ( $F_{2,30} = 150.736, p < 0.001, \eta^2 = 0.762$ ) (See Fig. 5). Additionally, significant interactions were found for  $W \times H$  ( $F_{4,60} = 6.481, p < 0.001, \eta^2 = 0.809$ ).

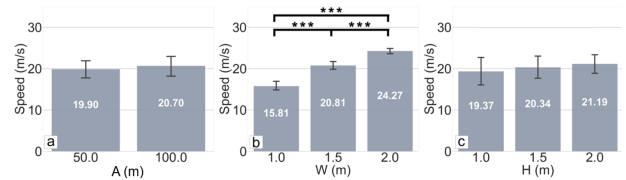


Figure 5: Average movement speeds for each factor. The error bars show 95% CIs(\* $p < 0.05$ , \*\* $p < 0.01$ , \*\*\* $p < 0.001$ )

##### 4.5.3 Steering Law Verification

Regression was utilized to fit the dataset we collected to the Euclidean Steering Law model, which accounted for the effects of path width and height within the 3D large screen (See Eq. (4)). The model's fitness was evaluated using the R-squared ( $R^2$ ) value, ranging from 0 to 1, where higher values indicate better fitness. Our findings revealed that the Weighted Euclidean model demonstrated strong fitness with our dataset ( $R^2 = 0.968$ ), where the coefficients were  $a = 0.339$ ,  $b = 0.055$ , and  $\eta = 0.296$ .



## 4.6 Discussion

### 4.6.1 The Applicability of Steering Law in Piloting Control Task (RQ1)

Our findings indicate a strong fit between the previous Steering Law model and the collected data, with  $R^2$  values reaching 0.968. This suggests that despite the shift in task complexity from 2D stylus steering to 3D third-person piloting, the model retains robust explanatory ability over user performance and behavior.

### 4.6.2 The effect of tunnel width and height (RQ2)

The findings suggest tunnel width and height had varying impacts on users' behaviors and performance, particularly concerning movement time and average movement speed. Specifically, the broader tunnel width and height lead to a shorter movement time and faster average movement speed. This trend is aligned with previous works that the spatial constraints represented by  $W$  [39, 2, 36]. The behavior pattern can be regarded as participants tend to adopt a more cautious strategy to pilot the aircraft as the height or width decreases.

Moreover, tunnel width exhibited a more pronounced influence compared to tunnel height on the results (see Fig. 4 and Fig. 5), which was further supported by the coefficient of  $\eta$ . In this regard, the weight of height ( $\eta = 0.296$ ) was significantly lower than the default value of width (1) [15]. This discrepancy can be attributed to the characteristics of tasks and mechanisms of interactivity. Specifically, the tunnel was designed to be straight in this experimental setting. Thus, during the piloting process, the participants mostly controlled the left joystick, which was utilized to control the movement (forward, backward, left, and right) of the aircraft (see Fig. 2). In contrast, they only adjusted the altitude of the aircraft (right joystick) when they wanted to avoid a collision with the internal wall of the tunnel, thus resulting in width having a significantly higher effect on user behavior than height. Furthermore, an intriguing behavioral pattern emerged during the experiment: participants tended to adjust the altitude even when encountering a broader tunnel height, despite the ability to navigate through the straight tunnel without altering altitude. We considered this behavioral pattern to be a safety strategy employed by users during the interaction, a phenomenon supported by previous studies on pedestrian behavior [7, 16]. It suggests that visual uncertainty and environmental noise tend to prompt individuals to maintain greater distances when walking. Similarly, participants tend to adopt a cautious approach to our task, preferring to expend additional effort to adjust height rather than risking no adjustment at all.

Additionally, due to the interactivity of aircraft piloting, we considered that different piloting trajectories may result in varying effects weights for width and height. For example, in this study, where the trajectory is a straight path, participants primarily adjust the direction (forward, backward, left, and right) of the aircraft rather than frequent altitude control. Consequently, height appears to have a weaker influence than width. Thus, for a better understanding in the following sections, in scenarios where width adjustments are more frequent than height, piloting the aircraft horizontally, we designate width as the **major effect axis** ( $M_e$ ) and height as the **minor axis** ( $m_e$ ). Conversely, when there is a greater need for height adjustments and fewer width refinements, piloting the aircraft vertically, we refer to height as the  $M_e$  and width as the  $m_e$ .

## 5 USER STUDY 2: PILOTING WITHIN THE COMPLEX SCENARIO

In Study 1 (See Sec. 4), we confirmed the spatial-constrained effect in immersive 3D piloting tasks. Our findings indicated that different spatial constraints result in varying weights between height and width. Consequently, we designated the width as the major effect axis ( $M_e$ ) and the height as the minor effect axis ( $m_e$ ) in our current straight trajectory condition. In this study, we aim to investigate

more complex scenarios, such as curved paths, to explore further the effects caused by spacial limitations (width and height) (RQ3).

### 5.1 Participants and Apparatus

We recruited 16 participants (8 females, 8 males) from a local university, aged between 18 and 26 years ( $M = 22.21, SD = 3.18$ ), who did not participate in the first user study. All participants reported clear vision and no prior experience with VR HMD, except for half who had 0-5 hours of weekly exposure. None of them had prior real-life aircraft/drone piloting experience, but they all had played similar games on PC. The same devices used in Study 1 were utilized to conduct this user study (See Sec. 4.2).

### 5.2 Design and Procedure

We employed a  $3 \times 3 \times 2 \times 7$  within-subjects design with four independent variables. Furthermore, we maintained consistency in the factors and their values from the first user study to ensure comparability. The independent variables included width, height, and length, with the addition of curvature radius with horizontal direction to the right as an extra factor, aligning the values with those used in a VR-based driving task [38], where larger radius of curvature represent approximately straight trajectories.

Moreover, to better control variables, we retained the absence of altitude adjustments in the piloting trajectory design for this study. Therefore, compared to Study 1, the tunnel in this study only incorporated the curvature radius while maintaining a consistent flight direction to the right, as previous work [38]. Thus, in Study 2, the major effect axis remains as width, while height remains as the minor effect axis. The conditions of this study are as follows: Effective Width ( $W$ ): 1m, 1.5m, and 2m; Effective Height ( $H$ ): 1m, 1.5m, and 2m; Movement Distance ( $A$ ): 50m, 100m and Curvature Radius( $R$ ): 32m, 64m, 129m, 517m, 1033m, 2067m, 4033m.

The procedures and interactive mechanisms used in this study mirrored those of Study 1 (See Sec. 4.4). Each participant spent nearly 40 minutes on the experiment, resulting in a total of 6048 successful trials without any collision between aircraft and the tunnel ( $3 W \times 3 H \times 7 R \times 2 A \times 16$  participants  $\times$  3 repetitions).

### 5.3 Results

After the experiment, a total of 6774 trials were collected, consisting of 6048 successful and 726 failures (10.7%). Following the exclusion of error trials, outliers (3.5%) exceeding or falling below the mean by more than three times the standard deviation were removed. Subsequently, the data underwent analysis using repeated-measures ANOVA (RM-ANOVA) with Bonferroni correction for post-hoc pairwise comparisons.

#### 5.3.1 Movement Time

As illustrated in Fig. 6, the main effects were found for  $W$  ( $F_{2,30} = 178.110, p < 0.001, \eta^2 = 0.116$ ),  $H$  ( $F_{2,30} = 17.213, p < 0.001, \eta^2 = 0.015$ ),  $A$  ( $F_{1,15} = 516.788, p < 0.001, \eta^2 = 0.221$ ), and  $R$  ( $F_{6,90} = 98.336, p < 0.001, \eta^2 = 0.126$ ). Significant interactions were found for  $W \times A$  ( $F_{2,30} = 16.608, p < 0.001, \eta^2 = 0.351$ ),  $H \times R$  ( $F_{12,180} = 2.434, p = 0.004, \eta^2 = 0.142$ ),  $W \times R$  ( $F_{12,180} = 16.964, p < 0.001, \eta^2 = 0.258$ ),  $A \times R$  ( $F_{6,90} = 45.745, p < 0.001, \eta^2 = 0.372$ ), and  $H \times A \times R$  ( $F_{12,180} = 2.541, p = 0.005, \eta^2 = 0.393$ ).

#### 5.3.2 Average Speed

We found significant main effects for  $W$  ( $F_{2,30} = 51.507, p < 0.001, \eta^2 = 0.255$ ),  $R$  ( $F_{6,90} = 54.826, p < 0.001, \eta^2 = 0.303$ ) and  $H$  ( $F_{2,30} = 0.876, p = 0.041, \eta^2 = 0.026$ ). Significant interaction effects were found for  $W \times A$  ( $F_{2,30} = 4.820, p = 0.008, \eta^2 = 0.256$ ),  $H \times R$  ( $F_{12,180} = 2.408, p = 0.004, \eta^2 = 0.330$ ),  $W \times R$

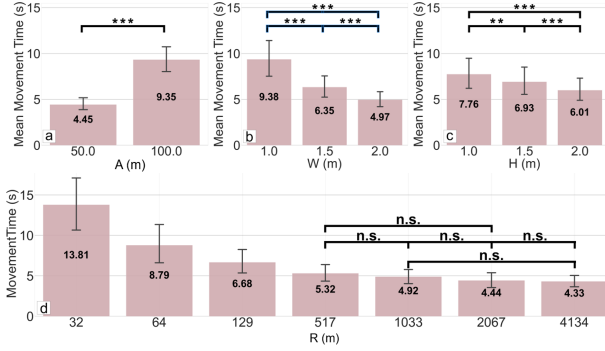


Figure 6: Movement times for each task parameter. The error bars show 95% CIs(\* $p < 0.05$ , \*\* $p < 0.01$ , \*\*\* $p < 0.001$ ). For Radius(d), all effects except for those denoted as “n. s.” were significant with  $p < 0.05$ , at least.

( $F_{12,180} = 5.520, p < 0.001, \eta^2 = 0.567$ ),  $A \times R$  ( $F_{6,90} = 3.226, p = 0.004, \eta^2 = 0.313$ ), and  $H \times W \times A \times R$  ( $F_{24,360} = 2.041, p = 0.002, \eta^2 = 0.577$ ).

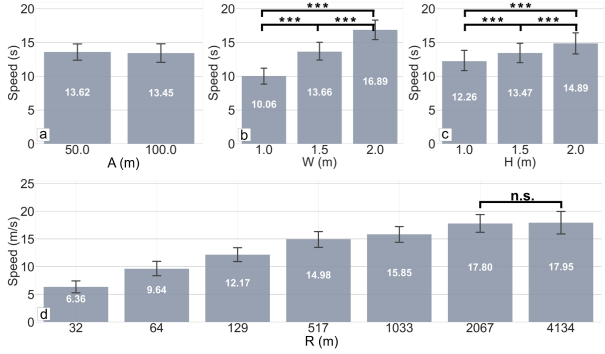


Figure 7: Average speed for each task parameter. The error bars show 95% CIs(\* $p < 0.05$ , \*\* $p < 0.01$ , \*\*\* $p < 0.001$ ). For Radius(d), all effects except for those denoted as “n. s.” were significant with  $p < 0.05$ , at least.

### 5.3.3 Model Fitting for each curvature radius

Considering the statistical main effects of curvature radius ( $R$ ) and the interaction effects between  $R$  and  $W$  and  $H$ , we employed the Euclidean Steering Law model to fit the movement time to explore the influence of  $W$  and  $H$  within different curvature radii. As depicted in Tab. 1, the weight value ( $\eta$ ) varied across different curvature radii, showing that the influence weight initially increased and then decreased with increasing curvature radius. To further investigate the relationship between  $R$  and  $\eta$ , we fitted the data using Log-normal distribution function (See Fig. 8). The R-squared values indicate that the weight value of the minor effect axis strictly follows the curve of Log-normal distribution ( $R^2 = 0.84$ ).

## 5.4 Discussion

### 5.4.1 The effect and relationship between curvature radius and spatial constraint (RQ3)

Based on the results obtained from this study, we initially demonstrated that curvature radius also influences user performance and behavioral patterns besides spatial constraints. Furthermore, the results of the RM-ANOVA statistically confirmed the main and interaction effects between curvature radius, width, and height. Sub-

R	Weighted Euclidean Steering Law model	$R^2$
32	$MT = -2.617 + 0.288\sqrt{0.093\left(\frac{A}{H}\right)^2 + \left(\frac{A}{W}\right)^2}$	0.954
64	$MT = -2.396 + 0.182\sqrt{0.251\left(\frac{A}{H}\right)^2 + \left(\frac{A}{W}\right)^2}$	0.915
129	$MT = -0.970 + 0.107\sqrt{0.659\left(\frac{A}{H}\right)^2 + \left(\frac{A}{W}\right)^2}$	0.909
517	$MT = -0.367 + 0.082\sqrt{0.553\left(\frac{A}{H}\right)^2 + \left(\frac{A}{W}\right)^2}$	0.969
1033	$MT = +0.298 + 0.069\sqrt{0.486\left(\frac{A}{H}\right)^2 + \left(\frac{A}{W}\right)^2}$	0.942
2067	$MT = -0.167 + 0.075\sqrt{0.268\left(\frac{A}{H}\right)^2 + \left(\frac{A}{W}\right)^2}$	0.952
4134	$MT = +0.729 + 0.059\sqrt{0.213\left(\frac{A}{H}\right)^2 + \left(\frac{A}{W}\right)^2}$	0.948

Table 1: Model fitting results for MT with Weighted Euclidean Steering Law

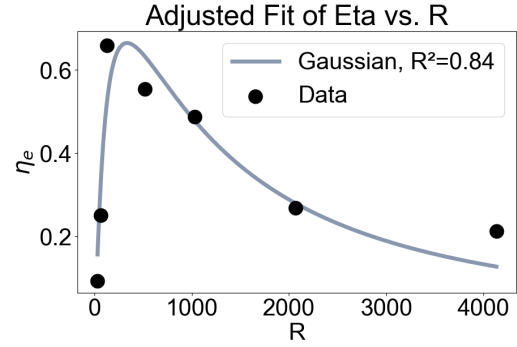


Figure 8: The fitting result between the weight value ( $\eta$ ) and Log-normal distribution function

sequently, we employed the weight of the Euclidean model to investigate the relationship between these different factors further.

The  $\eta$  values from the Euclidean model indicate that the  $\eta$  strongly fit the Log-normal distribution. Specifically, when the piloting trajectory reaches its maximum curvature radius or remains straight, the impact of height compared with width on user behavior is minimal. Conversely, as the curvature transitions from highly curved to straight, the significance of height progressively increases. We attribute this phenomenon to the changing proportion of effects between width and height. Specifically, in our current experimental setup, width serves as the main effect axis. Thus, when the curvature radius is large, and piloting trajectories tend towards straight lines, the impact of width significantly outweighs that of height, resulting in a relatively lower  $\eta$  value, which mirrors the results as discussed in Study 1 (See Sec. 4.6.2). Conversely, in highly curved trajectories, the influence of width peaks as participants have to continuously adjust lateral aircraft movement rather than altitude to avoid tunnel collisions. When the curvature radius is moderate, the importance of width and height becomes more balanced, leading to  $\eta$ , representing the weight of height, reaching its peak.

In summary, our results indicate that the effect of curvature radius on user behavior alters the weight of influence between width and height. Moreover, the weight coefficient ( $\eta$ ) on the minor axis fluctuates with the curvature radius, shifting from linear to curved trajectories and aligning with a normal distribution curve. This suggests that the existing model lacks applicability in scenarios with multiple curvature radii presented. Therefore, proposing a new model integrating curvature radius, width, and height effects becomes necessary for understanding users' piloting behavior and performance.

## 6 MODELING AND EVALUATION

Through Studies 1 and 2, we empirically demonstrated the applicability of the Steering Law in our piloting task (**RQ1**) and confirmed that the spatial constraints imposed by width and height exert varying effects on users' performance and behaviors (**RQ2**). We designated width and height as the major and minor effect axes, respectively, based on the characteristics of the piloting trajectory. Furthermore, we identified that the weight between width and height is not constant, fluctuating according to the curvature radius of the piloting trajectory (**RQ3**). Therefore, in this section, building upon the findings from RQ1-3, we aim to propose a new model capable of predicting users' piloting behavior and performance by considering the factors of width, height, length, and curvature radius (**RQ4**).

### 6.1 Modeling

As depicted in Sec. 2.1, among the models discussed, only the one proposed by Kattinakere et al. [15] takes into account the influence of spatial constraints, utilizing the coefficient  $\eta$  to represent the weight between width and height (See Eq. (4)). Therefore, building upon this model, we proposed an extended version with enhanced capabilities to elucidate users' behavioral patterns in complex piloting trajectories, including considerations for curvature radius.

Specifically, we first simplify the Euclidean model by removing the coefficient  $a$ , as previous works have shown that this intercept coefficient term does not significantly affect the final performance of the model [10, 28, 14]. Thus, the relationship between the movement time ( $MT_{eu}$ ) and the expression can be represented as:

$$\begin{aligned} MT_{eu} &\approx b \cdot \sqrt{\left(\frac{A}{W}\right)^2 + \eta \left(\frac{A}{H}\right)^2} \\ &= b \cdot A \cdot \sqrt{\left(\frac{1}{W}\right)^2 + \eta \left(\frac{1}{H}\right)^2} \end{aligned} \quad (7)$$

Then, leveraging the association between time, distance, and velocity ( $Time = \frac{A}{V}$ ), we can express Eq. (7) as:

$$V_{eu} = \frac{A}{MT_{eu}} = \frac{1}{b \cdot \sqrt{\left(\frac{1}{W}\right)^2 + \eta \left(\frac{1}{H}\right)^2}} \quad (8)$$

Additionally, considering the consistent linear relationship between curvature radius ( $R$ ) and velocity ( $V$ ), where  $V$  decreases with increasing curvature ( $\frac{1}{R}$ ) [28], we have:

$$V_R = c + d \cdot \frac{1}{R} \quad (9)$$

Where  $c$  and  $d$  are constants determined by linear regression. Drawing from the previous work [38], the speed caused by different factors can be accumulated as a weighted linear expression to represent the overall speed. Thus, the overall speed influenced by width, height, and curvature radius can be formulated as follows:

$$V_{all} = e + f \cdot V_{eu} + g \cdot V_R \quad (10)$$

Where  $e$ ,  $f$  and  $g$  is a constant. We can proceed to derive the total time required as follows:

$$MT_{all} = \frac{A}{V_{all}} = \frac{A}{e + f \cdot V_{eu} + g \cdot (c + d \cdot \frac{1}{R})} \quad (11)$$

Referring to Eq. (7), to keep the model from overfitting and to maintain simplicity, we hypothesize that the intercept coefficient ( $e + gc$ ) does not significantly impact the model's final performance. Therefore, when combining  $V_{eu}$  with  $V_R$ , we remove the intercept coefficient and extract the constant  $gd$  from the denominator from Eq. (11). Moreover, given that the weight value  $\eta$  follows a

Log-normal distribution curve, it is associated with the height factor, defined as the minor effect axis ( $m_e$ ). Therefore, our proposed candid model (**CM**) can be expressed as:

$$\begin{aligned} MT &= a \cdot \frac{1}{b \cdot \frac{A}{R} + \sqrt{\left(\frac{A}{M_e}\right)^2 + \eta_e \cdot \left(\frac{A}{m_e}\right)^2}} \\ \eta_e &= c \cdot \frac{1}{d \sqrt{2\pi}} \cdot \exp - \frac{1}{2} \left( \frac{\log(R) - e}{d} \right)^2 \end{aligned} \quad (12)$$

$A$ ,  $R$ ,  $M_e$ ,  $m_e$  represent the independent variable of path length, curvature radius, major effect axis, and minor effect axis. The  $a$ ,  $b$ ,  $c$ ,  $d$ , and  $e$  are coefficients determined by nonlinear regression.

### 6.2 Evaluation

To evaluate our proposed model, we conducted nonlinear regression and utilized two metrics: the Akaike Information Criterion (AIC) and R-square. Lower AIC values and higher R-square values generally indicate better model performance, suggesting stronger goodness of fit and explanatory power of independent variables on the dependent variable, respectively. Additionally, AIC helps prevent overfitting by penalizing model complexity, striking a balance between goodness of fit and model complexity.

The baseline (**BL**) chosen for comparison with our **CM** is the original Euclidean Model (See Eq. (4)), which is the only model considering the effect of both width and height. It is worth noting that other extended Steering Law models that only considered the effect of width cannot be applied in our scenario, as our study treats the height differently from the width [36, 38].

The data obtained from Study 2 ( $N = 126$ ) were utilized to fit the models. As described in Sec. 5.2, width was defined as the major effect axis ( $M_e$ ), while height was designated as the minor effect axis ( $m_e$ ). The results for AIC and R-square are illustrated in Tab. 2, which showed that our proposed model achieved 52.6% and 60.6% improvement in terms of AIC and R-square. To better understand the improvement of our proposed model, the fitting results between the observed and predicted values are visualized in Fig. 9).

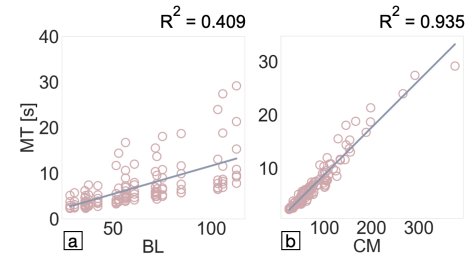


Figure 9: Model fitting for the original Euclidean model (a) and the model proposed in this work (b), with  $N=126$ .

### 6.3 Discussion

#### 6.3.1 The extended Steering Law model in piloting tasks (**RQ4**)

Building upon the findings from QR1-3, we introduced an extended Steering Law model that incorporates the impacts of spatial constraints (major and minor effect axes), length, and curvature radius in piloting tasks. We empirically and statistically assessed the effectiveness of our proposed model. The R-square and AIC metrics indicated that our model outperformed existing models, showcasing its superior performance.

Specifically, in comparison to the model applicable solely in straight spatial constraint piloting trajectory, our model integrated

Name	Model	Source	$R^2$	AIC	Coefficients				
BL	Eq. (4)	[15]	0.409	704.041	a = -0.781	b = 0.123	$\eta = 0.273$		
CM	Eq. (12)		<b>0.935</b>	<b>427.249</b>	a = 0.088	b = -18.482	c = 1.769	d = 1.146	e = 4.507

Table 2: Fitting results are presented, where 'BL' denotes the baseline and 'CM' represents our proposed candidate model. The values highlighted in bold signify superior performance.

only two additional coefficients, leading to at least a 52% enhancement, significantly enhancing the model's ability to interpret user behavioral patterns in the more complex context (such as curvature radius). Additionally, the AIC results suggest that the introduction of these coefficients does not increase the risk of overfitting, and the complexity they introduce remains suitable and acceptable. Furthermore, our model statistically confirmed the findings observed in Study 2, which indicated that the weight values attached to the minor axis followed the curve of Log-normal distribution. Leveraging this trend in our model, we demonstrated that it is inadequate, as in previous work [36], to include only curvature radius ( $R$ ) as an independent variable in this complex piloting task.

### 7 STUDY 3: MODEL VERIFICATION

Studies 1 and 2 predominantly focus on horizontal aircraft piloting scenarios, with  $M_e$  denoting width and  $m_e$  denoting height. To mitigate potential biases arising from horizontal movement, we introduced a new context, vertical aircraft piloting (upward), to validate our proposed model. The shift in orientation necessitated a redefinition of  $M_e$  and  $m_e$  because participants tend to adjust altitude more frequently than the direction vertically during the piloting process. Therefore, we reassigned height as  $M_e$  and width as  $m_e$ .

The study was conducted involving 8 participants (4 males and 4 females; Age  $M = 23.2$ ,  $SD = 2.54$ ) with 4 independent variables:  $W_e$  (2m, 3m, and 4m),  $H_e$  (2m, 3m, and 4m),  $A$  (50m, 100m), and  $R$  (64m, 129m, 517m, 1033m, and 2067m). The experiment utilized the same equipment, tasks, and procedures as studies 1 and 2. Following the experiment, a total of 2160 trials were collected ( $3 W \times 3 H \times 5 R \times 2 A \times 8$  participants  $\times$  3 repetitions). The collected data underwent the same preprocessing procedure as our previous studies to remove outliers (187 trails, 8.66%).

After the nonlinear regression between the data and our proposed model ( $n = 90$ ). Our model still maintains the high fitness ( $R^2 = 0.872$ ), which further confirms the applicability and efficacy of the model within various complex piloting tasks.

### 8 LIMITATIONS AND FUTURE WORK

In this study, we introduced a model aimed at understanding and predicting users' piloting behavior and performance. Despite its strengths, several limitations were identified and can serve as avenues for future research. First, although our model demonstrated good fitness across different piloting directions and orientations, it is currently limited to two standard directions (horizontal and vertical). Exploring additional movement directions, such as inclined trajectories with varying degrees, may result in different weightings of the effect between width and height. Therefore, future research will focus on investigating the weight values between height and width within diverse directions to validate the robustness of our model further. Second, we have only introduced tunnels and drones into the scene in our current setup. While this effectively controls variables and collects user behavior data within the experiments, it may not fully represent real-world scenarios, such as aerial combat games, where additional distractors are common. Some previous work has demonstrated that the existence of additional distractors may affect users' behavioral patterns and interactive strategies. Thus, further exploration of the effects of additional distractors will

be helpful in future research. Third, our experiments involved testing with virtual aircraft. Despite employing physics-based controls, we did not fully account for real-world factors such as air resistance and other physical interferences. Therefore, in future research, we intend to utilize real drone equipment to explore our findings further. Finally, while our user studies illustrated significant effects caused by the factors we researched, most participants were young individuals recruited from a local university. In the future, we intend to enrich our sample pool and increase the number of participants further to validate the reliability of our results across different populations.

### 9 CONCLUSION AND APPLICATION

We conducted three user studies to explore four questions about controlling moving objects like an aircraft in virtual reality (VR) and to model it. Study 1 aimed to investigate the effects of spatial constraints, specifically tunnel width and height, on users' performance and behavioral patterns during piloting tasks following a straight trajectory. The results revealed that piloting time could be effectively modeled using the extended Steering Law, which accounts for both width and height effects (**RQ1**). Furthermore, the findings indicated that width and height exerted different levels of impact on users' performance depending on the characteristics of the piloting trajectory (**RQ2**). We designated width as the major effect axis and height as the minor effect axis in the context of horizontal aircraft piloting. Subsequently, Study 2 explored the effects of spatial constraints in a more complex scenario involving curvature radius. Our results demonstrated that the weight value ( $\eta$ ) fluctuated with changes in curvature radius, following a Log-normal distribution pattern (**RQ3**). Consequently, the existing model tailored to straight trajectory piloting was not applicable to curved paths, prompting the development of a new model grounded in the Steering Law and findings from Studies 1-3. We fitted the data from Study 2 using our proposed model and compared it with the previous model, achieving improvements of 52.6% and 60.6% in terms of R-square and AIC metrics, respectively (**RQ4**). Finally, we revised the curvature and piloting orientation from horizontal to vertical to comprehensively evaluate the proposed model in Study 3. Despite these adjustments, the model exhibited a high fitness with an R-square value of 0.872.

To conclude, our studies and model offer practical guidance for game and interface designers to understand user behavior and optimize design. Furthermore, our model serves as a predictive tool, enabling designers to anticipate and evaluate difficulty levels before implementation for more informed design choices. For example, aerial combat game developers can adjust mission difficulty by modifying tunnel dimensions. Beyond gaming, in surgical training, our research helps practitioners manipulate robots in small, curved environments like patients' throats and intestines. This broader applicability highlights the value of our research in enhancing both virtual reality experiences and real-world precision tasks.

### ACKNOWLEDGMENT

We thank our participants for their time. This work is supported in part by the National Natural Science Foundation of China (#62207022).



## REFERENCES

- [1] Drone simulator for uas pilots. [www.dronesimpro.com](http://www.dronesimpro.com), 2024. Accessed: 2024-04-02. 3
- [2] J. Accot and S. Zhai. Beyond fitts' law: models for trajectory-based hci tasks. In *Proceedings of the ACM SIGCHI Conference on Human Factors in Computing Systems*, CHI '97, p. 295–302. Association for Computing Machinery, New York, NY, USA, 1997. doi: 10.1145/258549.258760 1, 2, 5
- [3] J. Accot and S. Zhai. Scale effects in steering law tasks. In *Proceedings of the SIGCHI Conference on Human Factors in Computing Systems*, CHI '01, p. 1–8. Association for Computing Machinery, New York, NY, USA, 2001. doi: 10.1145/365024.365027 4
- [4] D. Ahlström. Modeling and improving selection in cascading pull-down menus using fitts' law, the steering law and force fields. In *Proceedings of the SIGCHI conference on Human factors in computing systems*, pp. 61–70, 2005. 2
- [5] S. Bateman, A. Doucette, R. Xiao, C. Gutwin, R. L. Mandryk, and A. Cockburn. Effects of view, input device, and track width on video game driving. In *Proceedings of Graphics Interface 2011*, GI '11, p. 207–214. Canadian Human-Computer Communications Society, Waterloo, CAN, 2011. 1
- [6] R. Bretin, E. S. Cross, and M. Khamis. Co-existing with a drone: Using virtual reality to investigate the effect of the drone's height and cover story on proxemic behaviours. In *Extended Abstracts of the 2022 CHI Conference on Human Factors in Computing Systems*, CHI EA '22. Association for Computing Machinery, New York, NY, USA, 2022. doi: 10.1145/3491101.3519750 1
- [7] R. Cohen, J. Biddle, and D. Rosenbaum. Manual obstacle avoidance takes into account visual uncertainty, motor noise, and biomechanical costs. *Experimental Brain Research*, 201:587–592, 2010. doi: 10.1007/s00221-009-2042-8 3, 5
- [8] DJI Technology Co., Ltd., Shenzhen, Guangdong, China. *DJI Mini 2 User Manual*, 1.0 ed., June 2021. 3
- [9] DJI Technology Co., Ltd., Shenzhen, Guangdong, China. *DJI RC User Manual*, 1.0 ed., June 2022. 3
- [10] C. G. DRURY. Movements with lateral constraint. *Ergonomics*, 14(2):293–305, 1971. PMID: 5093722. doi: 10.1080/00140137108931246 2, 7
- [11] M. Endsley. Endsley, m.r.: Toward a theory of situation awareness in dynamic systems. *human factors journal* 37(1), 32–64. *Human Factors: The Journal of the Human Factors and Ergonomics Society*, 37:32–64, 03 1995. doi: 10.1518/001872095779049543 2
- [12] M. Endsley. Theoretical underpinnings of situation awareness: A critical review. *Situation awareness analysis and measurement*, pp. 3–32, 01 2000. 2
- [13] F. Gao, L. Wang, B. Zhou, X. Zhou, J. Pan, and S. Shen. Teach-repeat-replan: A complete and robust system for aggressive flight in complex environments. *IEEE Transactions on Robotics*, 36:1526–1545, 2019. doi: 10.1109/TRO.2020.2993215 2
- [14] E. R. Hoffmann. Review of models for restricted-path movements. *International Journal of Industrial Ergonomics*, 39(4):578–589, 2009. Special issue: Felicitating Colin G. Drury. doi: 10.1016/j.ergon.2008.02.007 7
- [15] R. S. Kattinakere, T. Grossman, and S. Subramanian. Modeling steering within above-the-surface interaction layers. In *Proceedings of the SIGCHI Conference on Human Factors in Computing Systems*, CHI '07, p. 317–326. Association for Computing Machinery, New York, NY, USA, 2007. doi: 10.1145/1240624.1240678 1, 2, 3, 5, 7, 8
- [16] A. Kiefer, R. Woods, and W. Warren. A behavioral dynamics approach to obstacle detection and avoidance by patients with tunnel vision. *Journal of Vision*, 13:482–482, 2013. doi: 10.1167/13.9.482 1, 3, 5
- [17] Y.-J. Ko, H. Zhao, Y. Kim, I. Ramakrishnan, S. Zhai, and X. Bi. Modeling two dimensional touch pointing. In *Proceedings of the 33rd Annual ACM Symposium on User Interface Software and Technology*, UIST '20, p. 858–868. Association for Computing Machinery, New York, NY, USA, 2020. doi: 10.1145/3379337.3415871 4
- [18] S. Kulikov, I. S. MacKenzie, and W. Stuerzlinger. Measuring the effective parameters of steering motions. In *CHI '05 Extended Abstracts on Human Factors in Computing Systems*, CHI EA '05, p. 1569–1572. Association for Computing Machinery, New York, NY, USA, 2005. doi: 10.1145/1056808.1056968 3
- [19] N. T. T. Le, H. Y. Zhu, and H.-T. Chen. Remote visual line-of-sight: A remote platform for the visualisation and control of an indoor drone using virtual reality. In *Proceedings of the 27th ACM Symposium on Virtual Reality Software and Technology*, VRST '21. Association for Computing Machinery, New York, NY, USA, 2021. doi: 10.1145/3489849.3489910 1
- [20] Z. Li, Y. Luo, J. Wang, et al. Feasibility and performance enhancement of collaborative control of unmanned ground vehicles via virtual reality. *Personal and Ubiquitous Computing*, 2024. doi: 10.1007/s00779-024-01799-4 2
- [21] L. Liu, R. V. Liere, and K. J. Kruszyński. Modeling the Effect of Force Feedback for 3D Steering Tasks. *Joint Virtual Reality Conference of EGVE - EuroVR*, p. 8 pages, 2011. Artwork Size: 8 pages ISBN: 9783905674330 Publisher: [object Object]. doi: 10.2312/EGVE/JVRC11/031-038 1
- [22] L. Liu, J.-B. Martens, and R. v. Liere. Revisiting path steering for 3D manipulation tasks. *International Journal of Human-Computer Studies*, 69(3):170–181, 2011. doi: 10.1016/j.ijhcs.2010.11.006 1, 2
- [23] Y. Luo, J. Wang, H.-N. Liang, S. Luo, and E. G. Lim. Monoscopic vs. stereoscopic views and display types in the teleoperation of unmanned ground vehicles for object avoidance. In *2021 30th IEEE International Conference on Robot & Human Interactive Communication (RO-MAN)*, pp. 418–425, 2021. doi: 10.1109/RO-MAN50785.2021.9515455 2
- [24] Y. Luo, J. Wang, Y. Pan, S. Luo, P. Irani, and H.-N. Liang. Teleoperation of a fast omnidirectional unmanned ground vehicle in the cyber-physical world via a vr interface. In *Proceedings of the 18th ACM SIGGRAPH International Conference on Virtual-Reality Continuum and Its Applications in Industry*, VRCAI '22. Association for Computing Machinery, New York, NY, USA, 2023. doi: 10.1145/3574131.3574432 2
- [25] Y. Luo, J. Wang, R. Shi, H.-N. Liang, and S. Luo. In-device feedback in immersive head-mounted displays for distance perception during teleoperation of unmanned ground vehicles. *IEEE Transactions on Haptics*, 15(1):79–84, 2022. doi: 10.1109/TOH.2021.3138590 2
- [26] B. Matusiak and B. Sudbø. Width or height? which has the strongest impact on the size impression of rooms? results from full-scale studies and computer simulations. *Architectural Science Review*, 51:165 – 172, 2008. doi: 10.3763/asre.2008.5120 1, 2
- [27] M. Montazer, C. Drury, and M. Karwan. An optimization model for self-paced tracking on circular courses. *IEEE Transactions on Systems, Man, and Cybernetics*, 18(6):908–916, 1988. doi: 10.1109/21.23090 2, 3
- [28] M. A. MONTAZER and C. G. DRURY. A test of the beggs' model for self-paced movements. *Ergonomics*, 32(5):497–511, 1989. doi: 10.1080/00140138908966120 2, 7
- [29] P. Monteiro, D. Carvalho, M. Melo, F. Branco, and M. Bessa. Application of the steering law to virtual reality walking navigation interfaces. *Computers & Graphics*, 77:80–87, 2018. doi: 10.1016/j.cag.2018.10.003 3
- [30] G. R. Postal, W. Pavan, and R. Rieder. A virtual environment for drone pilot training using vr devices. *2016 XVIII Symposium on Virtual and Augmented Reality (SVR)*, pp. 183–187, 2016. doi: 10.1109/SVR.2016.39 2
- [31] R. Senanayake and R. S. Goonetilleke. Pointing device performance in steering tasks. *Perceptual and Motor Skills*, 122(3):886–910, 2016. PMID: 27216944. doi: 10.1177/0031512516649717 1
- [32] A.-I. Slean, R.-D. Vatavu, and J. Vanderdonck. Taking that perfect aerial photo: A synopsis of interactions for drone-based aerial photography and video. In *Proceedings of the 2021 ACM International Conference on Interactive Media Experiences*, pp. 275–279, 2021. 2
- [33] X. Wang and K. Yan. Immersive human-computer interactive virtual environment using large-scale display system. *Future Gener. Comput. Syst.*, 96:649–659, 2017. doi: 10.1016/j.FUTURE.2017.07.058 1
- [34] Y. Wei, K. Xu, Y. Li, L. Yu, and H.-N. Liang. Exploring and modeling directional effects on steering behavior in virtual reality. *IEEE Transactions on Visualization and Computer Graphics*, 2024. 2
- [35] S. Yamanaka and H. Miyashita. Modeling the steering time difference

- between narrowing and widening tunnels. In *Proceedings of the 2016 CHI Conference on Human Factors in Computing Systems*, CHI '16, p. 1846–1856. Association for Computing Machinery, New York, NY, USA, 2016. doi: 10.1145/2858036.2858037 [2](#)
- [36] S. Yamanaka and H. Miyashita. Modeling pen steering performance in a single constant-width curved path. In *Proceedings of the 2019 ACM International Conference on Interactive Surfaces and Spaces*, ISS '19, p. 65–76. Association for Computing Machinery, New York, NY, USA, 2019. doi: 10.1145/3343055.3359697 [1](#), [2](#), [3](#), [5](#), [7](#), [8](#)
- [37] S. Yamanaka and W. Stuerzlinger. Modeling fully and partially constrained lasso movements in a grid of icons. In *Proceedings of the 2019 CHI Conference on Human Factors in Computing Systems*, CHI '19, p. 1–12. Association for Computing Machinery, New York, NY, USA, 2019. doi: 10.1145/3290605.3300350 [2](#)
- [38] S. Yamanaka, T. Takaku, Y. Funazaki, N. Seto, and S. Nakamura. Evaluating the Applicability of GUI-Based Steering Laws to VR Car Driving: A Case of Curved Constrained Paths. *Proceedings of the ACM on Human-Computer Interaction*, 7(ISS):430:93–430:113, Nov. 2023. doi: 10.1145/3626466 [1](#), [2](#), [3](#), [4](#), [5](#), [7](#)
- [39] S. Zhai, J. Accot, and R. Woltjer. Human Action Laws in Electronic Virtual Worlds: An Empirical Study of Path Steering Performance in VR. *Presence: Teleoperators and Virtual Environments*, 13(2):113–127, Apr. 2004. eprint: <https://direct.mit.edu/pvar/article-pdf/13/2/113/1624210/1054746041382393.pdf>. doi: 10.1162/1054746041382393 [1](#), [3](#), [5](#)